Magic angle in electron energy loss spectra: Relativistic and dielectric corrections

A. P. Sorini,[1] J. J. Rehr,[1] and Z. H. Levine[2]
[1]*Department of Physics, University of Washington, Seattle, Washington 98195, USA*
[2]*National Institute of Standards and Technology, Gaithersburg, Maryland 20899, USA*
(Received 16 November 2007; published 19 March 2008)

Recently, it has been demonstrated that a careful treatment of both longitudinal and transverse matrix elements in electron energy loss spectra can explain the mystery of relativistic effects on the *magic angle*. Here, we show that there is an additional correction of order $(Z\alpha)^2$, where Z is the atomic number and α the fine structure constant, which is not necessarily small for heavy elements. Moreover, we suggest that macroscopic electrodynamic effects can give further corrections which can break the sample independence of the magic angle.

DOI: 10.1103/PhysRevB.77.115126 PACS number(s): 68.37.−d, 34.80.Dp

I. INTRODUCTION

The title of this paper is in reference to a recent work by Jouffrey *et al.*[1] with the title "The Magic Angle: A Solved Mystery." The *magic angle* in electron energy loss spectroscopy (EELS) is a special value of the microscope collection angle α_c at which the measured spectrum "magically" becomes independent of the angle between the incoming beam and the sample "c axis." The mystery, in the context of 200 keV electron microscopy, is that standard semirelativistic quantum theory yields a ratio of the magic angle θ_M to "characteristic angle" θ_E of more than twice the observed[2] value. Unfortunately, time[3] and again,[2,4] the theoretical justification of the factor of 2 turned out to be an errant factor of 2 elsewhere in the calculation. A key contribution of Jouffrey *et al.* was the observation that relativistic "transverse" effects, when properly included in the theory, naturally give a factor of 2 correction to the nonrelativistic magic angle. Here, we show that there are yet additional corrections to the theory which can even break the sample independence of the magic angle.

As in Ref. 1, we consider here the problem of a relativistic probe electron scattering off of a macroscopic condensed matter sample. Similar problems have been solved long ago using both semiclassical[5] and fully quantum-mechanical approachs.[6–8] Indeed, the fully quantum-mechanical, relativistic case of scattering two plane-wave electrons has long been a textbook problem.[9,10] This classic problem was revived recently in the works of Jouffrey *et al.*[1] and Schattschneider *et al.*,[11] in which a "flaw" in the standard theory is pointed out. The flaw is the approximation that the so-called longitudinal and transverse matrix elements for the scattering process may be summed incoherently, as argued by Fano in a seminal paper.[7] In fact, this approximation is only valid when the sample under consideration posseses certain symmetries. In a later review paper,[8] Fano states this condition explicitly; namely, that his original formula for the cross section is only applicable to systems of cubic symmetry. However, this caveat seems to have been generally ignored and, hence, turns out to be the source of the magic angle "mystery."[1] Jouffrey *et al.*, and later Schattschneider *et al.*, showed that if one correctly sums and squares the transition matrix elements then, in the dipole approximation, one finds the magic angle corrected by a factor of 2.

Our aim here is to examine the theory in more detail in order to derive both relativistic and material-dependent corrections to the magic angle. In Sec. II, we consider relativistic electron scattering within the formalism of quantum electrodynamics (QED). Working in the Coulomb gauge, we show that one can almost reproduce the results of Jouffrey *et al.* and the theory of Schattschneider *et al.*, apart from a simple correction term of order $\hbar\omega/mc^2$, which is not always negligible. Here, $\hbar\omega$ is the energy lost by the probe, and mc^2 is the rest energy of an electron. In Sec. III, we suggest the possibility of incorporating macroscopic electrodynamic effects into the theory, which can break the symmetry of sample independence of the magic angle.

II. COULOMB GAUGE CALCULATION

An appealing aspect of the formalism of Schattschneider *et al.* is its simplicity. Their approach is similar to the semiclassical approach of Møller,[5] but with the added simplification of working with a probe and sample described by the Schrödinger equation, rather than the Dirac equation. They also find that the theory is simplified by choosing to work in the Lorentz gauge. Unfortunately, however, the theory of Møller is somewhat *ad hoc* in that a classical calculation in the Lorentz gauge is modified by replacing the product of two classical charge densities by the product of four different wave functions in order to obtain the transition matrix element. For the Møller case, this procedure is justified *a posteriori* by the fact that it reproduces the correct result, but is only rigorously justified by appealing to the method of second quantization.[9] Møller's procedure is physically reasonable *a priori*, because Møller was interested in the scattering of electrons in vacuum. However, the theory of Schattschneider *et al.*, which largely mimics Møller's theory, is less physically reasonable *a priori*, since the electrons are not scattering in vacuum, but are inside a solid which can screen the electrons. Nevertheless, since the discrepancy is small, the theory of Schattschneider *et al.* is justified *a posteriori* to a lesser extent by experiment.[2] We, thus, refer to the theory of Schattschneider *et al.* as a "vacuum-relativisitic theory." Consequently, in an effort to account for the discrepancy with experiment, we feel that it is useful to rederive the

results of Jouffrey *et al.* from a more fundamental starting point.

It is easy to see that the theory of Schattschneider *et al.* is not formally exact, though for many materials the error in the vacuum-relativistic limit is negligible. In fact, the discrepancy can be easily explained via single-particle quantum mechanics: although Schattschneider *et al.* work explicitly in the Lorentz gauge, they also make the assumption that the momentum and the vector potential commute,

$$\boldsymbol{p}\cdot\boldsymbol{A}(\boldsymbol{r})\overset{?}{=}\boldsymbol{A}(\boldsymbol{r})\cdot\boldsymbol{p}. \tag{1}$$

Of course, this commutation relation is only exact in the Coulomb gauge. In the end, however, the error in this approximation only affects the final results (e.g., matrix elements) by a correction of order $\hbar\omega/mc^2$ compared to unity, where $\hbar\omega$ is the energy lost by the probe. Since $\hbar\omega/mc^2$ is at most $(Z\alpha)^2$ for deep-core energy loss, the effect is usually negligible, except, of course, for very heavy atoms. To see how corrections such as the above enter into the theory, and to further determine whether or not such corrections are meaningful or simply artifacts of the various approximations used in the theory of Schattschneider *et al.*, we find it useful to present a fully quantum-mechanical, relativistic many-body treatment along the lines of Fano,[8] but without any assumption of symmetry of the sample. Our treatment is at least as general as that of Schattschneider *et al.* as far as the symmetry of the sample is concerned. Thus, going beyond the formulations of Schattschneider *et al.* and Møller, we take as our starting point the many-particle QED Hamiltonian. We then show that in a single-particle approximation, the theory yields the result of Schattschneider *et al.* together with the correction mentioned above.

Our starting point, therefore, is the Hamiltonian in Coulomb gauge[9]

$$H = H_{\mathrm{el}} + H_{\mathrm{int}} + H_{\mathrm{rad}}, \tag{2}$$

where the Hamiltonian has been split into three parts:

(i) the unperturbed electron part

$$H_{\mathrm{el}} = \int d^3x\,\psi^\dagger(\boldsymbol{x})(c\boldsymbol{\alpha}\cdot\boldsymbol{p} + \boldsymbol{\beta}mc^2)\psi(\boldsymbol{x}), \tag{3}$$

where $\psi(\boldsymbol{x})$ is the second-quantized Dirac field, $\boldsymbol{\alpha}_i$ and $\boldsymbol{\beta}$ are the usual Dirac matrices, m is the electron mass, and c is the speed of light;

(ii) the unperturbed (transverse) radiation part

$$H_{\mathrm{rad}} = \sum_{\boldsymbol{k}}\sum_{i=1}^{2} a^\dagger_{\boldsymbol{k},i}a_{\boldsymbol{k},i}\hbar\omega_k, \tag{4}$$

where $a_{\boldsymbol{k},i}$ destroys a photon of momentum $\boldsymbol{k}$, polarization $\boldsymbol{\epsilon}_{\boldsymbol{k},i}$, and energy $\hbar\omega_k$; and

(iii) the interaction part

$$H_{\mathrm{int}} = +e\int d^3x\,\psi^\dagger(\boldsymbol{x})\boldsymbol{\alpha}\cdot\boldsymbol{A}(\boldsymbol{x})\psi(\boldsymbol{x}),$$

$$+\frac{e^2}{2}\int d^3x d^3y\,\frac{\psi^\dagger(\boldsymbol{x})\psi^\dagger(\boldsymbol{y})\psi(\boldsymbol{y})\psi(\boldsymbol{x})}{|\boldsymbol{x}-\boldsymbol{y}|}, \tag{5}$$

where

$$\boldsymbol{A}(\boldsymbol{x}) = \sum_{\boldsymbol{k},i}\sqrt{\frac{2\pi\hbar c^2}{V\omega_k}}(a_{\boldsymbol{k},i}\boldsymbol{\epsilon}_{\boldsymbol{k},i}e^{i\boldsymbol{k}\cdot\boldsymbol{x}} + a^\dagger_{\boldsymbol{k},i}\boldsymbol{\epsilon}^*_{\boldsymbol{k},i}e^{-i\boldsymbol{k}\cdot\boldsymbol{x}}), \tag{6}$$

$e=|e|$ is the charge of the proton, and V is the system volume.

Let us next specialize to the case of a fixed number $(N+1)$ of electrons where the $(N+1)$th electron is singled out as the "fast probe" traveling with velocity $\boldsymbol{v}_0$, and the remaining N electrons make up the sample. We also introduce a lattice or cluster of ion cores (below we consider only elemental solids of atomic number Z, but the generalization to more complex systems is obvious) which is treated classically, and which gives rise to a potential $v_{\text{e-core}}(\boldsymbol{x})=\Sigma_{i=1}^{N/Z}(-Ze^2)/|\boldsymbol{x}-\boldsymbol{R}_i|$ as seen by the electrons. In this case, our Hamiltonian becomes

$$\begin{aligned}H = &\left[c\boldsymbol{\alpha}\cdot\left(\boldsymbol{p}+\frac{e}{c}\boldsymbol{A}(\boldsymbol{r})\right)+\boldsymbol{\beta}mc^2\right]+v_{\text{e-core}}(\boldsymbol{r})\\ &+\sum_{i=1}^{N}\left[c\boldsymbol{\alpha}^{(i)}\cdot\left(\boldsymbol{p}^{(i)}+\frac{e}{c}\boldsymbol{A}(\boldsymbol{r}^{(i)})\right)+\boldsymbol{\beta}^{(i)}mc^2\right]+e^2\sum_{i=1}^{N}\frac{1}{|\boldsymbol{r}-\boldsymbol{r}^{(i)}|}\\ &+\frac{e^2}{2}\sum_{1=i\neq j=1}^{N}\frac{1}{|\boldsymbol{r}^{(i)}-\boldsymbol{r}^{(j)}|}+\sum_{i=1}^{N}v_{\text{e-core}}(\boldsymbol{r}^{(i)})+v_{\text{core-core}}+H_{\mathrm{rad}},\end{aligned} \tag{7}$$

where the coordinates which are not labeled by an index refer to the probe electron. The interaction $v_{\text{core-core}}$ between ion cores is a constant and is henceforth dropped.

To proceed to a single-particle approximation for the sample, the interaction of the sample electrons among themselves and with the potential of the ion cores may be taken into account by introducing a single-particle self-consistent potential $v(\boldsymbol{x})$ which includes both $v_{\text{e-core}}(\boldsymbol{x})$ and exchange-correlation effects. The interaction of the probe electron with the effective single electron of the sample will be considered explicitly. The difference between this interaction and the actual interaction between the probe and sample can be accounted for by introducing another potential $v'(\boldsymbol{x})$ which is not necessarily the same as $v(\boldsymbol{x})$; $v'(\boldsymbol{x})$ is, in theory, "closer" to the pure $v_{\text{e-core}}(\boldsymbol{x})$ potential than $v(\boldsymbol{x})$ though, in practice, this difference may not be of interest (see the Appendix for further explanation of this point). The potential $v'(\boldsymbol{x})$ leads to diffraction of the probe electron, which will not be considered in this paper in order to make contact with the theory of Schattschneider *et al.* It is also for this reason that we have introduced a single-particle picture of the sample, along with the fact that we want to apply this theory to real condensed matter systems in a practical way. The extension to the many-body case, in which the only single-body potential

seen by the probe is due to the ion cores, is given in the Appendix. Thus, using the single-particle approximation for the sample,

$$H = \left\{ c\boldsymbol{\alpha} \cdot \left[\boldsymbol{p} + \frac{e}{c}\boldsymbol{A}(\boldsymbol{r}) \right] + \boldsymbol{\beta} mc^2 \right\} + \left\{ c\boldsymbol{\alpha}_s \cdot \left[\boldsymbol{p}_s + \frac{e}{c}\boldsymbol{A}(\boldsymbol{r}_s) \right] + \boldsymbol{\beta}_s mc^2 \right\} + v'(\boldsymbol{r}) + e^2 \frac{1}{|\boldsymbol{r} - \boldsymbol{r}_s|} + v(\boldsymbol{r}_s) + H_{\mathrm{rad}}, \tag{8}$$

where the quantities labeled by the letter s refer to the sample electron, and the unlabeled quantites refer to the probe electron. In the remainder of this paper, we set $v' \to 0$, though the generalization of the theory to include diffraction is not expected to be difficult.

As it turns out,[12] we may start from an effective Schrödinger treatment of both the sample *and the probe* rather than a Dirac treatment. The treatment of the probe by a "relativistically corrected" Schrödinger equation is standard practice[13] in much of EELS theory, and is appropriate[12] for modern microscope energies of interest here (e.g., a few hundred keV). The relativistic correction to the Schrödinger equation of the probe consists in simply replacing the mass of the probe m by the relativistic mass $m' = m\gamma$, where $\gamma = 1/\sqrt{1 - v_0^2/c^2}$. Moreover, working with a Schrödinger equation treatment facilitates contact with the "vacuum-relativistic" magic-angle theory of Schattschneider *et al.* We will indicate later how the results change if we retain a full Dirac treatment of the electrons. Thus, we may start with the Hamiltonian

$$\begin{aligned} H &= \frac{[\boldsymbol{p} + (e/c)\boldsymbol{A}(\boldsymbol{r})]^2}{2m'} + \frac{[\boldsymbol{p}_s + (e/c)\boldsymbol{A}(\boldsymbol{r}_s)]^2}{2m} \\ &\quad + v(\boldsymbol{r}_s) + \frac{e^2}{|\boldsymbol{r}_s - \boldsymbol{r}|} + H_{\mathrm{rad}} \\ &\equiv H_0 + \frac{e}{m'c}\boldsymbol{p} \cdot \boldsymbol{A}(\boldsymbol{r}) + \frac{e}{mc}\boldsymbol{p}_s \cdot \boldsymbol{A}(\boldsymbol{r}_s) + \frac{e^2}{|\boldsymbol{r}_s - \boldsymbol{r}_p|} + O(A^2). \end{aligned} \tag{9}$$

In this theory, the unperturbed states are then direct products of unperturbed sample electron states (which in calculations can be described, for example, by the computer code[14] FEFF8), unperturbed probe electron states (plane waves, ignoring diffraction), and the free (transverse) photon states. Also, from now on, we ignore the interaction terms which are $O(A^2)$. Thus, our perturbation is

$$U = \frac{e^2}{|\boldsymbol{r} - \boldsymbol{r}_s|} + \frac{e}{m'c}\boldsymbol{p} \cdot \boldsymbol{A}(\boldsymbol{r}) + \frac{e}{mc}\boldsymbol{p}_s \cdot \boldsymbol{A}(\boldsymbol{r}_s), \tag{10}$$

and we are interested in matrix elements of

$$U + UG_0U + \cdots, \tag{11}$$

where the one-particle Green's function is

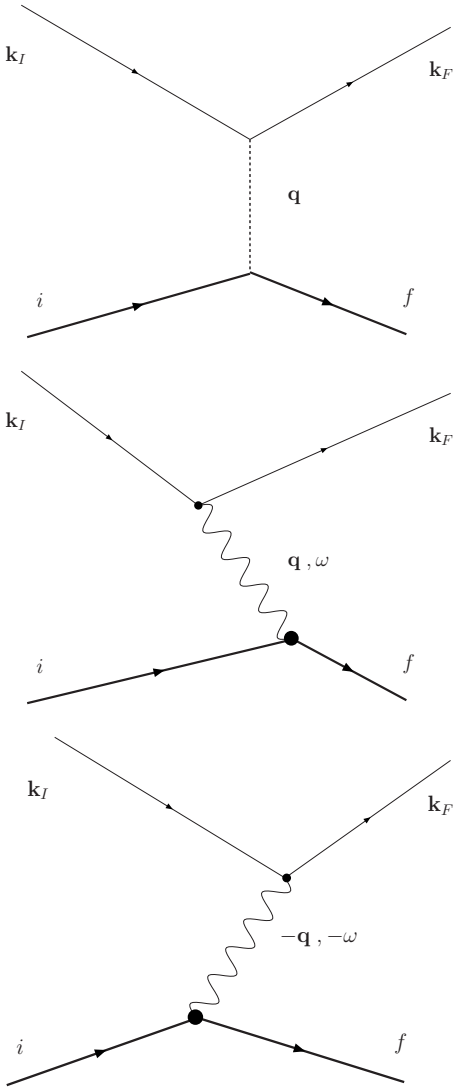

FIG. 1. Feynman diagrams for the scattering process due to both the instantaneous Coulomb interaction (upper) and the transverse photon interaction (middle, lower). The solid lines labeled by momenta $\mathbf{k}_I$ and $\mathbf{k}_F$ represent the probe particle; thick solid lines labeled by the letters i and f represent the sample particle; the dashed line is the instantaneous Coulomb interaction; and the wiggly lines are transverse photons. Time flows to the right.

$$G_0(E) = \frac{1}{E - H_0 + i\eta} \tag{12}$$

and η is a positive infinitesimal. The matrix elements are taken between initial and final states (ordered as probe, sample, photon)

$$|I\rangle = |k_I\rangle|i\rangle|0\rangle \quad \text{and} \quad |F\rangle = |k_F\rangle|f\rangle|0\rangle. \tag{13}$$

To lowest order (e^2) there will be a "longitudinal" (instantaneous Coulomb) contribution to the matrix element, and a transverse (photon mediated) contribution, as illustrated in Fig. 1.

Instead of elaborating the details from standard perturbation theory, we simply write down the result for the matrix element

$$M = \frac{4\pi e^2}{V}\left[\frac{1}{q^2}\langle f|e^{i\boldsymbol{q}\cdot\boldsymbol{r}_s}|i\rangle + \frac{1}{\omega^2 - c^2q^2}\frac{k_T^j}{m'}\langle f|\frac{p_s^j}{m}e^{i\boldsymbol{q}\cdot\boldsymbol{r}_s}|i\rangle\right], \tag{14}$$

where $\boldsymbol{k}_T$ (see Fig. 2) is the part of the initial (or final) momentum which is perpendicular to the momentum transfer $\hbar\boldsymbol{q}$. In the remainder of this paper, we will choose our units such that $\hbar = 1$.

$$k_T^j = \left(\delta_{lj} - \frac{q_l q_j}{q^2}\right)k_F^l = \left(\delta_{lj} - \frac{q_l q_j}{q^2}\right)k_I^l. \tag{15}$$

The result of Eq. (14) is easy to understand diagrammatically. For example, to each wiggly line of momentum $\boldsymbol{q}$ and energy ω, we may assign a value

$$\frac{1}{\omega - c|\boldsymbol{q}|}\left(\delta_{ij} - \frac{q_i q_j}{q^2}\right)\frac{2\pi c}{V|\boldsymbol{q}|}. \tag{16}$$

At this point, we note that the relativistic many-body version of Eq. (14) can be obtained by making intuitively reasonable replacements such as $\boldsymbol{p}/m \to c\alpha$, $e^{i\boldsymbol{q}\cdot\boldsymbol{r}_s} \to \Sigma_i e^{i\boldsymbol{q}\cdot\boldsymbol{r}^{(i)}}$. See the Appendix for further details.

Equation (14) is equivalent to the matrix elements given by Fano in Eq. (12) of Ref. 8. The cross section given by Fano in Eq. (16) of Ref. 8, in which the matrix elements have been summed incoherently, is not generally correct and is the source of the magic angle mystery.[11]

Before continuing to the dipole approximation, it is useful to rewrite Eq. (14) using the definition

$$\boldsymbol{k}_T = \boldsymbol{k}_I - \boldsymbol{q}\frac{\boldsymbol{q}\cdot\boldsymbol{k}_I}{q^2} \tag{17}$$

to eliminate $\boldsymbol{k}_T$ in favor of $\boldsymbol{k}_I$ (or, equivalently, $\boldsymbol{v}_0 = \boldsymbol{k}_I/m'$). Making this replacement, we obtain

$$M = \frac{4\pi e^2}{V}\left[\frac{1}{q^2}\langle f|e^{i\boldsymbol{q}\cdot\boldsymbol{r}}|i\rangle - \frac{\boldsymbol{q}\cdot\boldsymbol{v}_0}{mq^2}\frac{\langle f|\boldsymbol{q}\cdot\boldsymbol{p}e^{i\boldsymbol{q}\cdot\boldsymbol{r}}|i\rangle}{\omega^2 - c^2q^2} + \frac{\langle f|\boldsymbol{v}_0\cdot(\boldsymbol{p}/m)e^{i\boldsymbol{q}\cdot\boldsymbol{r}}|i\rangle}{\omega^2 - c^2q^2}\right], \tag{18}$$

which can be rewritten as

$$M = \frac{4\pi e^2}{V}\frac{1}{q^2 - (\omega^2/c^2)}\langle f|e^{i\boldsymbol{q}\cdot\boldsymbol{r}}\left[1 - \frac{\boldsymbol{v}_0\cdot\boldsymbol{p}}{mc^2} - \frac{\omega^2}{q^2c^2} \times\left(1 - \frac{\boldsymbol{q}\cdot\boldsymbol{p}}{m\omega}\right)\right]|i\rangle, \tag{19}$$

where we have made use of $\boldsymbol{q}\cdot\boldsymbol{v}_0 = \omega$ in order to cancel certain terms which appear after commuting the exponential through to the far left. Also, we have removed the label s from the position and momentum of the sample electron. This change in notation will be used throughout the remainder of this paper.

Equation (19) is the same as Eq. (6) of Schattschneider *et al.*, except for an "extra" term

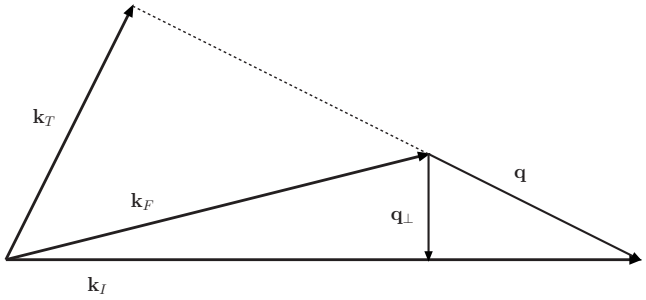

FIG. 2. The relevant momenta: $\boldsymbol{k}_I$ is the initial momentum of the probe particle, $\boldsymbol{k}_F$ is the final momentum of the probe particle, $\boldsymbol{q}$ is the momentum transfer $\boldsymbol{k}_I - \boldsymbol{k}_F$, and $\boldsymbol{k}_T$ is the part of both the initial and final momenta which is perpendicular to the momentum transfer.

$$\langle f|e^{i\boldsymbol{q}\cdot\boldsymbol{r}}\left(1 - \frac{\boldsymbol{q}\cdot\boldsymbol{p}}{m\omega}\right)|i\rangle. \tag{20}$$

Fortunately, this term may be simplified by considering the commutator

$$[e^{i\boldsymbol{q}\cdot\boldsymbol{r}}, H_0] = \left[e^{i\boldsymbol{q}\cdot\boldsymbol{r}}, \frac{p^2}{2m}\right] = e^{i\boldsymbol{q}\cdot\boldsymbol{r}}\left(-\frac{\boldsymbol{p}\cdot\boldsymbol{q}}{m} - \frac{q^2}{2m}\right), \tag{21}$$

where the first equal sign follows from the fact that $e^{i\boldsymbol{q}\cdot\boldsymbol{r}}$ commutes with everything in H_0 except for the kinetic term of the sample electron (by its definition, H_0 explicitly contains only local potentials). Then, using the fact that for any operator O,

$$\langle f|[O, H_0]|i\rangle = \langle f|O|i\rangle(E_i - E_f) = \langle f|O|i\rangle(-\omega), \tag{22}$$

we have

$$\langle f|e^{i\boldsymbol{q}\cdot\boldsymbol{r}}|i\rangle(-\omega) = -\langle f|e^{i\boldsymbol{q}\cdot\boldsymbol{r}}\left(\frac{\boldsymbol{p}\cdot\boldsymbol{q}}{m} + \frac{q^2}{2m}\right)|i\rangle \tag{23}$$

and, thus,

$$\langle f|e^{i\boldsymbol{q}\cdot\boldsymbol{r}}\left(1 - \frac{\boldsymbol{p}\cdot\boldsymbol{q}}{m\omega}\right)|i\rangle = \langle f|e^{i\boldsymbol{q}\cdot\boldsymbol{r}}\frac{q^2}{2m\omega}|i\rangle. \tag{24}$$

Making the above replacement in Eq. (19), we find

$$M = \frac{4\pi e^2}{V}\frac{1}{q^2 - \omega^2/c^2}\langle f|e^{i\boldsymbol{q}\cdot\boldsymbol{r}}\left(1 - \frac{\boldsymbol{v}_0\cdot\boldsymbol{p}}{mc^2} - \frac{\omega^2}{q^2c^2}\frac{q^2}{2m\omega}\right)|i\rangle \tag{25}$$

and we see that the extra term only changes the result by order ω/mc^2, where mc^2 is the rest energy of an electron and ω is the energy lost;

$$M = \frac{4\pi e^2}{V}\frac{1}{q^2 - \omega^2/c^2}\langle f|e^{i\boldsymbol{q}\cdot\boldsymbol{r}}\left(1 - \frac{\boldsymbol{v}_0\cdot\boldsymbol{p}}{mc^2} - \frac{\omega}{2mc^2}\right)|i\rangle = \frac{4\pi e^2}{V}\frac{1}{q^2 - \omega^2/c^2}\langle f|e^{i\boldsymbol{q}\cdot\boldsymbol{r}}\left(1 - \frac{\boldsymbol{v}_0}{mc^2}\cdot\left(\boldsymbol{p} + \frac{\boldsymbol{q}}{2}\right)\right)|i\rangle. \tag{26}$$

Equation (26) is the same as what Schattschneider *et al.*

would have obtained if they had not neglected the commutator $[\boldsymbol{p},\boldsymbol{A}]$.

That a term proportional to $\boldsymbol{p}+\boldsymbol{q}/2$ rather than simply $\boldsymbol{p}$ appears in Eq. (26) is correct and can be understood from the following simple example: The interaction Hamiltonian for a point particle with an external field is given by $e\phi - e\boldsymbol{v}\cdot\boldsymbol{A}/c$, or rather

$$H_{\text{int}} \sim \int d^3x \left(n(\boldsymbol{x})\phi(\boldsymbol{x}) - \frac{1}{c}\boldsymbol{j}(\boldsymbol{x})\cdot\boldsymbol{A}(\boldsymbol{x}) \right), \tag{27}$$

where $n(\boldsymbol{x})$ is the density and $\boldsymbol{j}(\boldsymbol{x})$ is the current, and where the above integral, with the potentials considered as functions of the source location, is a convolution in space and, thus, a product in Fourier space—the rough correspondence indicated by the "~" symbol in Eq. (27) is considered more rigourously in the Appendix. Next, we note that the Fourier transform of the current density (in second quantization) is given for a free particle by[15]

$$\boldsymbol{j}(\boldsymbol{q}) = \frac{1}{mV}\sum_{\boldsymbol{k}} \left(\boldsymbol{k} + \frac{\boldsymbol{q}}{2} \right) c^{\dagger}_{\boldsymbol{k}+\boldsymbol{q}} c_{\boldsymbol{k}}, \tag{28}$$

where

$$\psi(\boldsymbol{x}) = \sum_{\boldsymbol{k}} c_{\boldsymbol{k}} e^{i\boldsymbol{k}\cdot\boldsymbol{x}}, \tag{29}$$

and where $\boldsymbol{q}$ is considered to be the momentum transferred *to* the sample. This is in agreement with the usual conventions of EELS

$$\boldsymbol{q} = \boldsymbol{k}_I - \boldsymbol{k}_F. \tag{30}$$

Thus, we see that Eq. (26) is indeed correct, in both sign and magnitude of the extra term.

Dipole approximation and the magic angle

In the dipole approximation, Eq. (26) reduces to

$$\frac{4\pi e^2}{V}\frac{1}{q^2-\omega^2/c^2}\langle f|\left(i\boldsymbol{q}\cdot\boldsymbol{r} - \frac{\boldsymbol{v}_0\cdot\boldsymbol{p}}{mc^2} \right)|i\rangle. \tag{31}$$

The term $(1-\boldsymbol{v}_0\cdot\boldsymbol{q}/2mc^2)$ does not contribute because $\langle i|f\rangle = 0$. Now, we make use of the replacement $\boldsymbol{p}/m \to i\omega\boldsymbol{r}$ which is appropriate within the matrix element to find

$$\frac{4\pi e^2}{V}\frac{i}{q^2-\omega^2/c^2}\langle f|\left(\boldsymbol{q} - \frac{\boldsymbol{v}_0(\boldsymbol{q}\cdot\boldsymbol{v}_0)}{c^2} \right)\cdot\boldsymbol{r}|i\rangle. \tag{32}$$

We have, thus, found the same "shortened q vector" that appears in Eq. (15) of Schattschneider *et al.* and Eq. (2) of Jouffrey *et al.* Specifically, for an initial electron velocity $\boldsymbol{v}_0$ in the z direction, we have found the replacement $q_z \to q_z(1-v_0^2/c^2)$ which, in turn, leads to a significant correction (on the order of 100% for typical electron microscopes) to the magic angle.

The magic angle θ_M is defined for materials with a c axis by the equality of two functions of collection angle α_c:

$$F(\alpha_c) \equiv \int_0^{\alpha_c} d\theta\theta \frac{\theta^2}{[\theta^2+\theta_E^2/\gamma^4]^2} \tag{33}$$

and

$$G(\alpha_c) \equiv 2\frac{\theta_E^2}{\gamma^4}\int_0^{\alpha_c} d\theta\theta \frac{1}{[\theta^2+\theta_E^2/\gamma^4]^2}, \tag{34}$$

where $\gamma=(1-v_0^2/c^2)^{-1/2}$, θ_E is the so-called characteristic angle given in terms of the energy loss ω, the initial probe speed v_0, and $k_I\theta_E=\omega/v_0$. Both of the above integrals may easily be evaluated in terms of elementary functions, but we leave them in the above form for comparison with the theory of Sec. III. Equations (33) and (34) both make use of the approximation $\sin(\theta)\approx\theta$. Since typical scattering angles are on the order of milliradians, this small angle approximation is highly accurate.

The expressions for $F(\alpha_c)$ and $G(\alpha_c)$ are easily derived within the framework of the Schattschneider "vacuum theory"[11] and result in a ratio of magic angle to characteristic angle which is independent of the material which makes up the sample. The factors of $(1-v_0^2/c^2)$ which appear in Eqs. (33) and (34) come from including the transverse effects (as in Sec. I) and, thus, the nonrelativistic $(c\to\infty)$ result for the ratio of magic angle to characteristic angle is independent of transverse effects. The transverse correction to the magic angle is on the order of 100%. This corrected theoretical magic angle is in much better agreement with the experimentally observed magic angle, although the experimentally observed magic angle seems be somewhat larger (on the order of 30%) and sample dependent.[2] These further discrepancies between theory and experiment are addressed in Sec. III.

III. MACROSCOPIC ELECTRODYNAMIC EFFECTS

As discussed above, the result of Schattschneider *et al.* is nearly in agreement with that obtained in Sec. II of this paper in the vacuum-relativistic limit. However, because of the residual discrepancy between these results and experiment, we now consider how macroscopic electrodynamic effects can be incorported into the quantum-mechanical single-particle formalism. We find that the corrections to the magic angle which result can be quite substantial at low energy loss. However, we are unaware of any experimental data in this regime with which to compare the theory. Nevertheless, the inclusion of dielectric response introduces a sample dependence of the theoretical magic angle which is consistent with the sign of the observed discrepancy.

Certain condensed matter effects are already present in the existing formalism via the behavior of the initial and final single-particle states in the sample, and in many-electron effects which are neglected in the independent electron theory. However, the macroscopic response of the sample can be taken into account straightforwardly within a dielectric formalism. This procedure is similar to the well-known "matching" procedure between atomic calculations and macroscopic-dielectric calculations of the stopping power.[16–18] That is, the fast probe may interact with many atoms at once, as long as the condition $v_0 \gg \omega_0 a$ (where ω_0 is

a typical electronic frequency and a a typical length scale) is fulfilled. Under these conditions, the sample can be treated using the electrodynamics of continuous media.[16]

Effects due to the macroscopic response of the system can be included within a formalism that parallels that of Schattschneider *et al.* simply by choosing the "generalized Lorentz gauge"[16] for a given dielectric function $\epsilon(\omega)$, instead of the Lorentz gauge of the vacuum-relativistic theory. In the generalized Lorentz gauge, most of the formal manipulations of Schattschneider *et al.* carry through in the same way, except that instead of Eq. (19) we end up with

$$M = \frac{4\pi e^2}{\epsilon(\omega) V} \frac{1}{q^2 - \epsilon(\omega)\omega^2/c^2} \langle f | e^{i\boldsymbol{q}\cdot\boldsymbol{r}} \left[1 - \frac{\epsilon(\omega)\boldsymbol{v}_0}{mc^2} \cdot \left(\boldsymbol{p} + \frac{\boldsymbol{q}}{2} \right) \right] | i \rangle . \tag{35}$$

The factors of ϵ in Eq. (35) can be understood physically as due to the fact that $c \to c/\sqrt{\epsilon}$ in the medium, and also to the fact that the sample responds to the electric field $\boldsymbol{E}$ rather than the electric displacement $\boldsymbol{D}$. Equation (35) is derived in the following section.

Generalized Lorentz gauge calculation

We consider a probe electron which passes through a continuous medium characterized by a macroscopic frequency-dependent dielectric constant $\epsilon(\omega)$ and magnetic permeability $\mu = 1$. It is appropriate to ignore the spatial dispersion of the dielectric constant at this level of approximation.[19] Then Maxwell's equations are

$$\nabla \cdot \boldsymbol{D} = 4\pi \rho_{\text{ext}}, \tag{36}$$

with $\boldsymbol{D} = \epsilon \boldsymbol{E}$, and

$$\nabla \times \boldsymbol{B} = \frac{4\pi \boldsymbol{j}_{\text{ext}}}{c} + \frac{1}{c}\frac{\partial \boldsymbol{D}}{\partial t}, \tag{37}$$

where the charge and current densities ρ_{ext} and $\boldsymbol{j}_{\text{ext}}$ refer only to the "external" charge and current for a probe electron shooting through the material at velocity $\boldsymbol{v}_0$. The other two Maxwell equations refer only to $\boldsymbol{E}$ and $\boldsymbol{B}$, and can be satisfied exactly using the definitions

$$\boldsymbol{E} = -\nabla\phi - \frac{1}{c}\frac{\partial \boldsymbol{A}}{\partial t} \tag{38}$$

and

$$\boldsymbol{B} = \nabla \times \boldsymbol{A}. \tag{39}$$

We next insert Eqs. (38) and (39) into Eqs. (36) and (37) and choose the generalized Lorentz gauge[16]

$$\nabla \cdot \boldsymbol{A} + \frac{1}{c}\frac{\partial}{\partial t} \int dt' \, \epsilon(t - t') \phi(t') = 0. \tag{40}$$

This gauge choice leads to the momentum space $(\boldsymbol{q}, \omega)$ equations

$$\left[-q^2 + \epsilon(\omega)\frac{\omega^2}{c^2} \right] \phi(\boldsymbol{q}, \omega) = 4\pi \frac{\rho_{\text{ext}}(\boldsymbol{q}, \omega)}{\epsilon(\omega)} \tag{41}$$

and

$$\left[-q^2 + \epsilon(\omega)\frac{\omega^2}{c^2} \right] \boldsymbol{A}(\boldsymbol{q}, \omega) = 4\pi \frac{\boldsymbol{j}_{\text{ext}}(\boldsymbol{q}, \omega)}{c}. \tag{42}$$

We now write $\rho_{\text{ext}}(\boldsymbol{q}, \omega) = (-2\pi e)\delta(\omega - \boldsymbol{q}\cdot\boldsymbol{v}_0)$ and $\boldsymbol{j}_{\text{ext}} = \boldsymbol{v}_0 \rho_{\text{ext}}$ to find explicit expressions for ϕ and $\boldsymbol{A}$:

$$\epsilon(\omega)\phi(\boldsymbol{q}, \omega) = \frac{4\pi(-2\pi e)\delta(\omega - \boldsymbol{q}\cdot\boldsymbol{v}_0)}{[\epsilon(\omega)\omega^2/c^2] - q^2} \tag{43}$$

and

$$\boldsymbol{A}(\boldsymbol{q}, \omega) = \frac{\boldsymbol{v}_0}{c}\epsilon(\omega)\phi(\boldsymbol{q}, \omega). \tag{44}$$

Then, proceeding roughly in analogy with Schattschneider *et al.*, we have

$$\begin{aligned} H &= H_0 + \frac{e}{2mc}(\boldsymbol{p}\cdot\boldsymbol{A} + \boldsymbol{A}\cdot\boldsymbol{p}) - e\phi + O(A^2) \\ &= H_0 + \frac{e}{2mc}(2\boldsymbol{A}\cdot\boldsymbol{p} - i\nabla\cdot\boldsymbol{A}) - e\phi + O(A^2). \end{aligned} \tag{45}$$

Next, evaluating the perturbation $U \equiv H - H_0$ with $\boldsymbol{A} = (\boldsymbol{v}_0/c)\epsilon(\omega)\phi$, we find

$$U = \frac{e}{mc}\left(\phi\frac{\epsilon(\omega)}{c}\boldsymbol{v}_0\cdot\boldsymbol{p} - i\epsilon\frac{\boldsymbol{v}_0}{2c}\cdot\nabla\phi \right) - e\phi. \tag{46}$$

In calculating the matrix element of U, it is appropriate to replace $\nabla\phi$ by $i\boldsymbol{q}\phi$ for the case when the final states are on the *left* in the matrix element. Thus,

$$\begin{aligned} M \equiv \langle f | \langle k_f | U | k_i \rangle | i \rangle &= -e\phi(\boldsymbol{q}, \omega) \langle f | e^{i\boldsymbol{q}\cdot\boldsymbol{r}} \\ &\times \left[1 - \frac{\epsilon(\omega)}{mc^2}\boldsymbol{v}_0 \cdot \left(\frac{\boldsymbol{p} + \boldsymbol{q}}{2} \right) \right] | i \rangle . \end{aligned} \tag{47}$$

Alternatively, since

$$\phi(\boldsymbol{q}, \omega) = \frac{-4\pi e}{\epsilon(\omega)(q^2 - \omega^2\epsilon(\omega)/c)}, \tag{48}$$

we have

$$M = \frac{4\pi e^2}{\epsilon(\omega)(q^2 - \epsilon(\omega)\omega^2/c^2)} \langle f | e^{i\boldsymbol{q}\cdot\boldsymbol{r}} \left[1 - \frac{\epsilon(\omega)}{mc^2}\boldsymbol{v}_0 \cdot \left(\frac{\boldsymbol{p} + \boldsymbol{q}}{2} \right) \right] | i \rangle . \tag{49}$$

In the dipole approximation, Eq. (49) reduces to

$$\frac{4\pi e^2}{\epsilon(\omega) V} \frac{1}{q^2 - \epsilon(\omega)\omega^2/c^2} \langle f | i \left[\boldsymbol{q} - \epsilon(\omega)\frac{\boldsymbol{v}_0(\boldsymbol{q}\cdot\boldsymbol{v}_0)}{c^2} \right] \cdot \boldsymbol{r} | i \rangle, \tag{50}$$

where $\epsilon(\omega)$ is the generally complex valued macroscopic dielectric constant which can be calculated, for example, by the FEFFOP code.[20] Consequently, we find that instead of the longitudinal q-vector replacement

$$q_z \to q_z(1 - \beta^2) \tag{51}$$

found by Jouffrey *et al.* and Schattschneider *et al.*, we obtain the replacement

$$q_z \to q_z[1 - \epsilon(\omega)\beta^2], \tag{52}$$

which is appropriate for an electron traversing a continuous dielectric medium. In the same way that Eq. (51) can be understood classically as being due to a charge in uniform motion in vacuum,[21] Eq. (52) can be understood as due to a charge in uniform motion in a medium. Because the motion is uniform, the time dependence can be eliminated in favor of a spatial derivative opposite to the direction of motion and multiplied by the speed of the particle. For motion in the z direction,

$$\frac{\partial}{\partial t} \to -v_0 \frac{\partial}{\partial z}. \tag{53}$$

Therefore, if we consider the electric field

$$\boldsymbol{E} = -\nabla\phi - \frac{1}{c}\frac{\partial \boldsymbol{A}}{\partial t} \to -\nabla\phi + \frac{v_0}{c}\frac{\partial \boldsymbol{A}}{\partial z}, \tag{54}$$

Eq. (51) follows from the substitution $A_z=(v_0/c)\phi$, whereas Eq. (52) follows by making the correct substitution in the presence of a medium

$$A_z = \frac{v_0}{c}\epsilon\phi, \tag{55}$$

which in Fourier space gives

$$\boldsymbol{E}(\boldsymbol{q},\omega) = \left[-i\boldsymbol{q} + \hat{z}\frac{\epsilon(\omega)v_0^2}{c^2}iq_z\right]\phi(\boldsymbol{q},\omega), \tag{56}$$

which is equivalent to Eq. (52).

Because Eq. (52) depends on the macroscopic-dielectric function, the ratio θ_M/θ_E, which formerly was a function only of v_0, will now show material dependence. This is seen from the generalization of Eqs. (33) and (34), the equality of which gives the magic angle. Instead of Eq. (33) for $F(\alpha_c)$, we now have

$$F(\alpha_c) \equiv \int_0^{\alpha_c} d\theta\theta \frac{\theta^2}{|\theta^2 + \theta_E^2 g|^2}, \tag{57}$$

and instead of Eq. (34), we now have

$$G(\alpha_c) \equiv 2\theta_E^2|g|^2 \int_0^{\alpha_c} d\theta\theta \frac{1}{|\theta^2 + \theta_E^2 g|^2}, \tag{58}$$

where

$$g = 1 - \epsilon(\omega)v_0^2/c^2 \tag{59}$$

is a complex number which replaces $1/\gamma^2$ in the vacuum-relativistic theory.

If one can calculate the macroscopic dielectric function of the sample by some means,[20] then the material-dependent magic angle can be determined theoretically and compared to experiment. Furthermore, the correction to the magic angle given by the introduction of the macroscopic-dielectric constant relative to the relativistic macroscopic "vacuum value" of Jouffrey *et al.* is seen to be typically positive (since $\mathrm{Re}[\epsilon] \lesssim 1$ and $0 \lesssim \mathrm{Im}[\epsilon]$), in rough agreement with observation.[2] In fact, it turns out that the correction is always positive for the materials we consider, and is substantial only for low energy loss where the dielectric function differs substantially from its vacuum value. For modern EELS experiments which use relativistic microscope energies and examine low energy loss regions, the effect of the dielectric correction on the magic angle should be large.

Example calculations using our relativistic dielectric theory compared to both the relativistic vacuum theory of Schattschneider *et al.* and to the nonrelativistic vacuum theory are shown in Fig. 3 for the materials boron nitride and graphite. The data of Daniels *et al.*[2] is also shown in the figures. We have not attempted to estimate the true error bars for the data; the error bars in the figure indicate only the error resulting from the unspecified finite convergence angle.

IV. CONCLUSIONS

We have developed a fully relativistic theory of the magic angle in electron energy loss spectra starting from the QED Hamiltonian of the many-body system. As with the single-particle theory of Jouffrey *et al.* and Schattschneider *et al.*, we find a factor of 2 transverse correction to the nonrelativistic ratio θ_M/θ_E. We have also shown how macroscopic electrodynamic effects can be incorporated into the relativistic single-particle formalism of Schattschneider *et al.* In particular, we predict that these dielectric effects can be important for determining the correct material-dependent magic angle at low energy loss, where the difference between the dielectric function relative to its vacuum value is observed to be substantial.

Several other factors may be important for correctly describing the energy loss dependence of the magic angle in anisotropic materials. In particular, we believe that further study of the many-body effects (beyond a simple macroscopic-dielectric model) via explicit calculations of the *microscopic-dielectric* function and including time-dependent density functional–Bethe-Salpeter theory[22] is an important next step in the description of all EELS phenomena, including the magic angle.

ACKNOWLEDGMENTS

We wish to thank K. Jorrisen for helpful comments and encouragement. This work is supported by the National Institute of Standards and Technology (NIST) Grant No. 70 NAMB 2H003 (A.P.S.) and the Department of Energy (DOE) Grant No. DE-FG03-97ER45623 (J.J.R.), and was facilitated by the DOE Computational Materials Science Network.

APPENDIX: RELATIVISTIC EFFECTS

Starting from Eq. (7) we write (the notation H_0 in the Appendix differs from that in the main text):

$$H_0 = c\boldsymbol{\alpha}\cdot\boldsymbol{p} + \boldsymbol{\beta}mc^2 + v_{\text{e-core}}(\boldsymbol{r}) + \sum_{i=1}^{N}[c\boldsymbol{\alpha}^{(i)}\cdot\boldsymbol{p}^{(i)} + \boldsymbol{\beta}^{(i)}mc^2 + v_{\text{e-core}}(\boldsymbol{r}^{(i)})] + \frac{1}{2}\sum_{1=i\neq j=1}^{N}\frac{e^2}{|\boldsymbol{r}^{(i)} - \boldsymbol{r}^{(j)}|} + H_{\text{rad}} \tag{A1}$$

and

$$U = e\boldsymbol{\alpha}\cdot\boldsymbol{A}(\boldsymbol{r}) + \sum_{i=1}^{N}\frac{e^2}{|\boldsymbol{r}-\boldsymbol{r}^{(i)}|} + \sum_{i=1}^{N} e\boldsymbol{\alpha}^{(i)}\cdot\boldsymbol{A}(\boldsymbol{r}^i). \quad \text{(A2)}$$

We are interested in matrix elements of the perturbation

$$U + UG_0U + \cdots \quad \text{(A3)}$$

between eigenstates of the unperturbed Hamiltonian

$$|I\rangle = |k_i\rangle|\Psi_i\rangle|0\rangle \quad \text{and} \quad |F\rangle = |k_f\rangle|\Psi_f\rangle|0\rangle. \quad \text{(A4)}$$

The difference between the many-body case and the single-particle theory of the sample is that the wave function of the sample now depends on N electron coordinates, instead of one effective coordinate. Also, we see that the only potential "seen" by the probe (i.e., included in the unperturbed probe Hamiltonian) is the $v_{\text{e-core}}$ potential. This is to be contrasted with the "unperturbed" sample Hamiltonian which includes not only the $v_{\text{e-core}}$ but also the Coulomb interactions between all the sample electrons.

Consequently, working with a unit volume and proceeding exactly as in the single-particle case, we find a longitudinal contribution to the matrix element

$$M_L = \frac{4\pi e^2}{q^2}u^{\dagger}(\boldsymbol{k}_f)u(\boldsymbol{k}_i)\langle\Psi_f|\sum_{i=1}^{N} e^{i\boldsymbol{q}\cdot\boldsymbol{r}^{(i)}}|\Psi_i\rangle \quad \text{(A5)}$$

and a transverse contribution

$$M_T = \frac{4\pi e^2}{\omega^2/c^2 - q^2}u^{\dagger}(\boldsymbol{k}_f)\boldsymbol{\alpha}_T u(\boldsymbol{k}_i)\cdot\langle\Psi_f|\sum_{i=1}^{N}\boldsymbol{\alpha}^{(i)}e^{i\boldsymbol{q}\cdot\boldsymbol{r}^{(i)}}|\Psi_i\rangle, \quad \text{(A6)}$$

where

$$\boldsymbol{\alpha}_T = \boldsymbol{\alpha} - \boldsymbol{q}\frac{\boldsymbol{q}\cdot\boldsymbol{\alpha}}{q^2}, \quad \text{(A7)}$$

and where the $u(\boldsymbol{p})$ are the usual free-particle Dirac spinors, normalized such that

$$u^{\dagger}(\boldsymbol{p})u(\boldsymbol{p}) = 1. \quad \text{(A8)}$$

The two matrix elements M_L and M_T are to be summed and then squared, but before proceeding with this plan, we make the following useful definitions: The transverse Kronecker delta function (transverse to momentum transfer)

$$\delta_T^{ij} = \delta^{ij} - \frac{q^i q^j}{q^2}; \quad \text{(A9)}$$

the (Fourier transformed) density operator

$$n(\boldsymbol{q}) = \sum_{i}^{N} e^{-i\boldsymbol{q}\cdot\boldsymbol{r}^{(i)}}; \quad \text{(A10)}$$

and the (Fourier transformed) current operator

$$\boldsymbol{j}(\boldsymbol{q}) = \sum_{i}^{N} c\boldsymbol{\alpha}^{(i)}e^{-i\boldsymbol{q}\cdot\boldsymbol{r}^{(i)}}. \quad \text{(A11)}$$

Next, we recall some properies of the Dirac spinors $u(\boldsymbol{p})$ and of Dirac matrices which we will presently find useful:

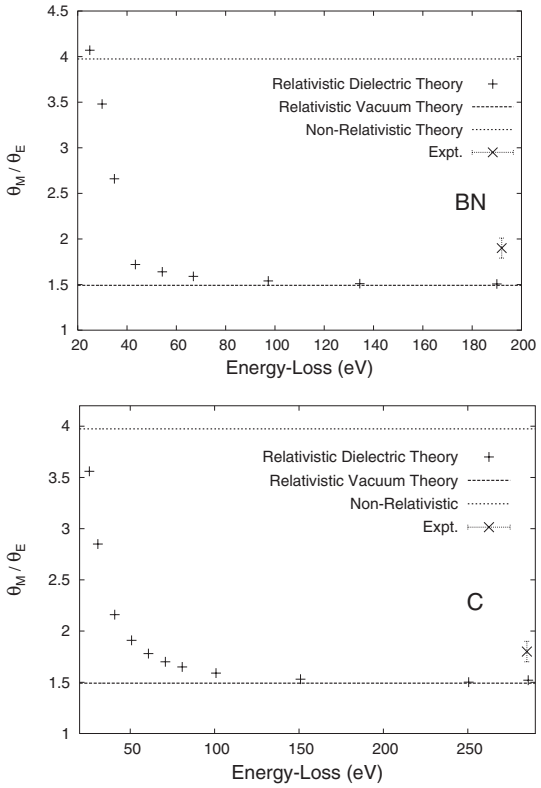

FIG. 3. The magic angle to characteristic angle ratio θ_M/θ_E is compared for three differing theories and one experiment (Ref. 2). The materials considered in the figure are boron nitride (top figure) and graphite (bottom). The microscope voltage is fixed at 195 keV. Both the nonrelativistic and relativistic vacuum theories show no dependence on the energy loss and no dependence on the material. The relativistic dielectric theory shows that the magic angle should deviate from the vacuum value by a significant amount in regions where the macroscopic dielectric response is substantial.

(i) There are four independent spinors $\{u^{(1)}, u^{(2)}, u^{(3)}, u^{(4)}\}$, the first two of which will refer to positive energy solutions, and the second two of which will refer to negative energy solutions (and are not used in this calculation).

(ii) The positive energy spinors satisfy a "spin sum"

$$\sum_{s=1}^{2} u^{(s)}(\boldsymbol{p})u^{(s)^{\dagger}}(\boldsymbol{p}) = \frac{1}{2E(p)}[E(p) + c\boldsymbol{\alpha}\cdot\boldsymbol{p} + \boldsymbol{\beta}mc^2]$$

$$\equiv \frac{1}{2E(p)}[E(p) + h_D(\boldsymbol{p})], \quad \text{(A12)}$$

where $E(p) = \sqrt{p^2c^2 + m^2c^4}$.

(iii) The Dirac matrices satisfy the trace identities

$$\mathrm{Tr}(\boldsymbol{\alpha}_i\boldsymbol{\alpha}_j) = 4\delta_{ij}, \quad \text{(A13)}$$

$$\mathrm{Tr}(\boldsymbol{\alpha}_i\boldsymbol{\alpha}_j\boldsymbol{\alpha}_k\boldsymbol{\alpha}_l) = 4(\delta_{ij}\delta_{kl} - \delta_{ik}\delta_{jl} + \delta_{il}\delta_{jk}), \quad \text{(A14)}$$

$$\mathrm{Tr}(\boldsymbol{\alpha}_T^i\boldsymbol{\alpha}^j) = \mathrm{Tr}(\boldsymbol{\alpha}_T^i\boldsymbol{\alpha}_T^j) = 4\delta_T^{ij}, \quad \text{(A15)}$$

$$\mathrm{Tr}(\boldsymbol{\alpha}^i\boldsymbol{\alpha}_T^j\boldsymbol{\alpha}^k\boldsymbol{\alpha}_T^l) = 4(\delta_T^{ij}\delta_T^{kl} - \delta^{ik}\delta_T^{jl} + \delta_T^{il}\delta_T^{jk}). \quad \text{(A16)}$$

(iv) Finally, we note that in this calculation, there are many simplifications due to the fact that $\omega \ll mc^2 < E(\boldsymbol{k}_I) \approx E(\boldsymbol{k}_F)$. For example,

$$\frac{1}{2E_iE_j}(E_iE_j + m^2c^4 + c^2\boldsymbol{k}_i \cdot \boldsymbol{k}_j) = 1 - \frac{\omega}{E(k_i)} + O\left(\frac{\omega^2}{E(k_i)^2}\right) \approx 1.$$

Throughout the calculation, we ignore terms of order $\omega/E(\boldsymbol{p}_I)$. Using these identities, it is easy to see that

$$\frac{1}{2}\sum_{s_i=1}^{2}\sum_{s_f=1}^{2}|M_L|^2 = \left(\frac{4\pi e^2}{q^2}\right)^2 |\langle \Psi_F|n_q^\dagger|\Psi_I\rangle|^2, \tag{A17}$$

which has the same form as in the nonrelativistic case (up to order ω/E_i); the squared matrix element is much simplified by the sum over final probe spin and average over initial probe spin. Of course, the matrix element itself is completely general in terms of probe spin, but many simplifications arise from ignoring the probe spin and exploiting the spin sums.

Continuing on to the transverse matrix element—and including a few more of the details (a, b, c, and d are Dirac indices)—we find

$$\begin{aligned}\frac{1}{2}\sum_{s_i=1}^{2}\sum_{s_f=1}^{2}|M_T|^2 &= \frac{1}{2}\sum_{s_i=1}^{2}\sum_{s_f=1}^{2}\left(\frac{4\pi e^2}{\omega^2/c^2 - q^2}\right)^2 u(\boldsymbol{k}_f)_a^{(s_f)*}\boldsymbol{\alpha}_T^{mab}u(\boldsymbol{k}_i)_b^{(s_i)}u(\boldsymbol{k}_i)_c^{(s_i)*}\boldsymbol{\alpha}_T^{ncd}u(\boldsymbol{k}_f)_d^{(s_f)}\langle\Psi_F|j_m(\boldsymbol{q})^\dagger|\Psi_I\rangle\langle\Psi_I|j_n(\boldsymbol{q})|\Psi_F\rangle \\ &= \left(\frac{4\pi e^2}{\omega^2/c^2 - q^2}\right)^2 \langle\Psi_F|j_m(\boldsymbol{q})^\dagger|\Psi_I\rangle\langle\Psi_I|j_n(\boldsymbol{q})|\Psi_F\rangle \mathrm{Tr}\{[E(k_f) + h_D(\boldsymbol{k}_f)]\boldsymbol{\alpha}_T^m[E(k_i) + h_D(\boldsymbol{k}_i)]\boldsymbol{\alpha}_T^n\} \\ &= \left(\frac{4\pi e^2}{\omega^2/c^2 - q^2}\right)^2 \left|\langle\Psi_I|\frac{\boldsymbol{v}_T \cdot \boldsymbol{j}(\boldsymbol{q})}{c^2}|\Psi_F\rangle\right|^2.\end{aligned} \tag{A18}$$

For the cross term, we find

$$\frac{1}{2}\sum_{s_i=1}^{2}\sum_{s_f=1}^{2}M_LM_T^* = (4\pi e^2)^2\frac{1}{q^2(\omega^2/c^2 - q^2)}\langle\Psi_F|n^\dagger(\boldsymbol{q})|\Psi_I\rangle \times\langle\Psi_I|\frac{\boldsymbol{j}(\boldsymbol{q}) \cdot \boldsymbol{v}_T}{c^2}|\Psi_F\rangle. \tag{A19}$$

Thus, we have finally derived an expression for the relativistic many-body summed-then-squared matrix elements summed and averaged over spins,

$$\begin{aligned}\frac{1}{2}\sum_{s_i}\sum_{s_f}|M_L + M_T|^2 &= \left(\frac{4\pi e^2}{V}\right)^2\left|\frac{\langle\Psi_I|n(\boldsymbol{q})|\Psi_F\rangle}{q^2} + \frac{\langle\Psi_I|\boldsymbol{v}_T \cdot \boldsymbol{j}(\boldsymbol{q})|\Psi_F\rangle}{\omega^2 - q^2c^2}\right|^2 \\ &= \left[\frac{4\pi e^2}{V(\omega^2/c^2 - q^2)}\right]^2\left|\langle\Psi_I|n(\boldsymbol{q}) - \frac{\boldsymbol{v}_0 \cdot \boldsymbol{j}(\boldsymbol{q})}{c^2}|\Psi_F\rangle\right|^2.\end{aligned} \tag{A20}$$

The last equality follows from

$$\boldsymbol{q} \cdot \langle\Psi_I|\boldsymbol{j}(\boldsymbol{q})|\Psi_F\rangle = \omega\langle\Psi_I|n(\boldsymbol{q})|\Psi_F\rangle, \tag{A21}$$

which itself follows by considering the commutator analogous to that of Eq. (21).

The final line of Eq. (A20) is quite pleasing since we have found that if we can "ignore" the spin of the probe particle, we may as well have started by taking matrix elements between electronic states only of the much simpler interaction Hamiltonian

$$U' = \int d^3x\left[n(\boldsymbol{x})\phi_\omega(\boldsymbol{x} - \boldsymbol{x}_p) - \frac{\boldsymbol{j}(\boldsymbol{x}) \cdot \boldsymbol{A}_\omega(\boldsymbol{x} - \boldsymbol{x}_p)}{c}\right], \tag{A22}$$

where the fields $\{\phi_\omega, \boldsymbol{A}_\omega\}$ are just the $e^{-i\omega t}$ components of the classical field of a point charge of velocity $\boldsymbol{v}_0$ in the Lorentz gauge, and where

$$n(\boldsymbol{x}) = \sum_i^N \delta(\boldsymbol{x} - \boldsymbol{x}^{(i)}) \tag{A23}$$

and

$$\boldsymbol{j}(\boldsymbol{x}) = \sum_i^N c\boldsymbol{\alpha}^{(i)}\delta(\boldsymbol{x} - \boldsymbol{x}^{(i)}). \tag{A24}$$

That is, if we take Eq. (A22) as our starting point and proceed in the usual way, we will find that our squared matrix elements are exactly the same as what we know to be correct from Eq. (A20). The photons have dropped out entirely.

[1] B. Jouffrey, P. Schattschneider, and C. Hebert, Ultramicroscopy **102**, 61 (2004).
[2] H. Daniels, A. Brown, A. Scott, T. Nichells, B. Rand, and R. Brydson, Ultramicroscopy **96**, 523 (2003).
[3] A. T. Paxton, M. van Schilfgaarde, M. Mackenzie, and A. J. Craven, J. Phys.: Condens. Matter **12**, 729 (2000).
[4] C. Hebert, B. Jouffrey, and P. Schattschneider, Ultramicroscopy **101**, 271 (2004).
[5] C. M. Møller, Ann. Phys. **14**, 531 (1932).
[6] H. A. Bethe, Ann. Phys. **5**, 325 (1930). This paper is reviewed in Ref. 23.
[7] U. Fano, Phys. Rev. **102**, 385 (1956).
[8] U. Fano, Annu. Rev. Nucl. Sci. **13**, 1 (1963).
[9] W. Heitler, *The Quantum Theory of Radiation*, 3rd ed. (Clarendon, Oxford, 1954).
[10] M. E. Peskin and D. V. Schroeder, *An Introduction to Quantum Field Theory* (Westview, Boulder, CO, 1995).
[11] P. Schattschneider, C. Hebert, H. Franco, and B. Jouffrey, Phys. Rev. B **72**, 045142 (2005).
[12] K. Fujiwara, J. Phys. Soc. Jpn. **16**, 2226 (1961).
[13] L.-M. Peng, S. Dudarev, and M. Whelan, *High-Energy Electron Diffraction and Microscopy* (Oxford University Press, New York, 2004).
[14] A. L. Ankudinov, B. Ravel, J. J. Rehr, and S. D. Conradson, Phys. Rev. B **58**, 7565 (1998).
[15] G. D. Mahan, *Many-Particle Physics* (Plenum, New York, 1981).
[16] L. D. Landau, E. M. Lifshitz, and L. P. Pitaevskii, *Electrodynamics of Continuous Media*, 2nd ed. (Permagon, New York, 1984).
[17] J. M. Fernández-Varea, F. Salvat, M. Dingfelder, and D. Liljequist, Nucl. Instrum. Methods Phys. Res. B **229**, 187 (2005).
[18] A. P. Sorini, J. J. Kas, J. J. Rehr, M. P. Prange, and Z. H. Levine, Phys. Rev. B **74**, 165111 (2006).
[19] E. Cockayne and Z. H. Levine, Phys. Rev. B **74**, 235107 (2006).
[20] M. Prange, G. Rivas, J. Rehr, and A. Ankudinov (unpublished).
[21] E. Fermi, Phys. Rev. **57**, 485 (1940).
[22] A. L. Ankudinov, Y. Takimoto, and J. J. Rehr, Phys. Rev. B **71**, 165110 (2005).
[23] M. Inokuti, Rev. Mod. Phys. **43**, 297 (1971).